NEUMAN ALUMINIUM

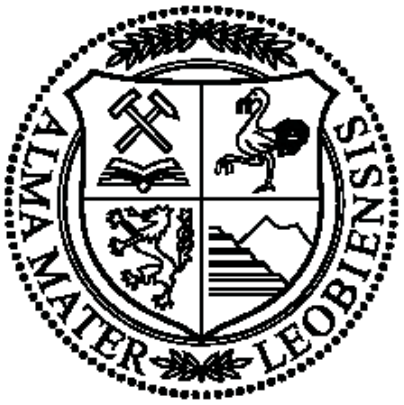

MASTERARBEIT

Natural aging of aluminum alloy 6082

Maximilian Karl Engelhart, BSc

Eidesstattliche Erklärung

Ich erkläre an Eides statt, dass die vorliegende Arbeit von mir selbstständig erstellt wurde und andere als die angegebenen Quellen nicht benutzt und die den Quellen inhaltlich und wörtlich entnommenen Stellen als solche erkenntlich gemacht wurden.

Leoben, August 2018

Maximilian Engelhart, BSc

Abstract

The aim of this thesis is to evaluate the effect of different heat treatments (pre aging) and pre deformation on the properties of 5 different aluminum alloys (6261, 6082 low alloyed, 6082 high alloyed, 6060 and 6066).

The different properties investigated such as aging response, precipitation behavior, mechanic and corrosion properties were microstructure (TEM), corrosion behavior and mechanical testing by tensile specimen.

The further understanding of the kinetics of natural aging and its influence on artificial aging can help to further improve the different heat treatments applied in aluminum industry. Natural aging behavior is important because it has a big influence on the kinetics of Artificial Aging (AA).

Natural aging proceeds through the decomposition of solid solution. Usually the decomposition stops when the first Guinier-Preston (GP) zones are formed. Formation of zones is common for many types of natural aging in different metals. The first separation of phases normally appears during natural aging.
If there is a high supersaturation of atoms and vacancies the formation of GP zones rapidly proceeds. However this is not wanted in some cases. Therefore methods need to be developed to inhibit effects of natural aging.

Therefore it is necessary to analyze the effect of different heat treatments on the final microstructure by TEM. Also mechanical properties and corrosion are greatly affected by the microstructure. Two different pre aging treatments with 30 min at 100°C and 3 hours at 140°C were applied and combined with different natural aging times between solution heat treatment with quenching, pre aging and artificial aging. The duration of artificial aging was 9 and 14 hours at 160°C.
It can be observed that the microstructure is strongly influenced by the heat treatment (pre aging in this case).

Kurzfassung

Das Ziel dieser Arbeit ist, den Effekt unterschiedlicher Voralterung und Vorverformung auf die Eigenschaften fünf unterschiedlicher Aluminiumlegierungen (6261, 6082low, 6082high, 6060, 6066) zu untersuchen.

Die untersuchten Eigenschaften sind Mikrostruktur (TEM), Korrosion und mechanische Eigenschaften durch Zugversuche. Mithilfe der gemessenen Werte kann die Auswirkung der natürlichen Alterung sowie der bestimmten Wärmebehandlungen besser eingeschätzt werden und dadurch Prozesse verbessert werden.

Ein besseres Verständnis der Kinetik der natürlichen Alterung sowie deren Einfluss auf die künstliche Alterung kann helfen Wärmebehandlungen in der Aluminiumindustrie weiter zu verbessern. Mit TEM Untersuchungen wurde die Wirkung unterschiedlicher Wärmebehandlungen auf die Mikrostruktur bestimmt.

Natürliche Alterung beschreibt die fortschreitende Auflösung des übersättigten Mischkristalls. Normalerweise endet diese mit der Bildung der ersten Guinier-Preston (GP) Zonen. Die Bildung von GP Zonen ist besonders bedeutend für Aluminium. Die ersten GP Zonen entstehen während der natürlichen Alterung.

Wenn der nach dem Abschrecken entstandene Mischkristall stark übersättigt ist und viele Leerstellen enthält entstehen rasch erste GP Zonen. In manchen Prozessen ist dies nicht erwünscht weil dadurch die Kinetik der Auslagerung bei erhöhten Temperaturen beeinflusst wird und dadurch ev. schlechtere mechanische Kennwerte hervorgerufen werden. Aus diesem Grund werden Methoden gesucht um die natürliche Alterung zu verlangsamen oder gänzlich zu verhindern.

Um die unterschiedlichen Wärmebehandlungen zu analysieren wurden die Mikrostrukturen im TEM untersucht. Die Mikrostruktur beeinflusst auch die mechanischen Eigenschaften und Korrosion in hohem Maße.

Es wurden zwei unterschiedliche Voralterungsbehandlungen (Pre Aging) angewandt:

- 3 Stunden 140°C
- 30 Minuten 100°C

Zwischen Lösungsglühen mit Abschrecken, Voralterung und Auslagern (9/14 Stunden bei 160°C) wurden entweder 10 Minuten oder eine Woche natürliche Alterung angewandt.

Weiters wurde mit Vorverformung durch Walzen versucht die natürliche Alterung zu unterdrücken.

Preface

This master thesis was written in spring and summer 2018 in cooperation with Neuman Aluminium, NTNU Trondheim and Montanuniversität Leoben.

I would like to thank Alexander Wimmer and Neuman Aluminium Fliesspresswerk for this thesis.

For the TEM investigations at NTNU Trondheim I would like to thank Randi Holmestad, Calin Mariora and Jonas Sunde.

Finally I would like to thank Bruno Buchmayr from Montanuniversität Leoben for supervising this thesis.

Table of contents

1. Introduction

Many studies have been done on the influence of artficial aging on various aluminum alloys.

With the experiments done in this thesis we try to influence the kinetics of natural aging in order to improve the performance of artificial aging.

In aluminum industry there is always natural aging between different heat treatments such as solution heat treatment with quenching and artfifical aging.

During the natural aging first clusters rich in alloying elements and so Guinier Preston zones are formed. The formation of this zones has a high influence on the further development of the microstructure.

Pogatscher et al. have shown that trace elements such as tin can block vacancies and inhibit natural aging in lean aluminum alloys such as 6060.

However for the alloy 6082 with a higher content of silicon and magnesium it is not possible to inhibit natural aging with trace elements.

Studies have shown that interrupted quenching and pre aging can slow natural aging kinetics.

For this thesis different alloys were pre-aged with 100°C and 140°C after quenching and then natural aging was applied for about 10 minutes and one week before artificial aging. Also conditions with only natural aging (10 minutes and one week) were produced for further tests.

The next step was to measure and compare the machanical properties of the different conditions in order to select interesting conditions for the TEM.

With the TEM analysis it was possible to compare the microstructures of the selected conditions. All conditions showed needle shaped precipitates which are characteristic for 6xxx alloys. The length, cross section and number density was measured. Also the volume fraction of the precipitates could be calculated.

Finally the goal was to relate values measured with the TEM to mechanical properties from the tensile specimen.

2. Theoretical background

2.1 History of natural aging in aluminum

In 1901 Alfred Wilm discovered the age hardening of aluminum. This means that the hardness and tensile strength of a material increase with time until a constant value is reached after a certain time.

The first aluminum alloy that used precipitation hardening was invented in 1906 by Alfred Wilm in Germany. The alloy is called duralumin. Duralumin contains 4% copper, 0,5% magnesium, and 0,5% manganese. It was discovered that the hardness would continually increase when left at room temperature after quenching. The hardness increase is caused by the creation of fine precipitates during natural aging. With the introduction of this alloy it was possible to use aluminum for high stressed technical constructions. [Wikipedia: Duralumin]

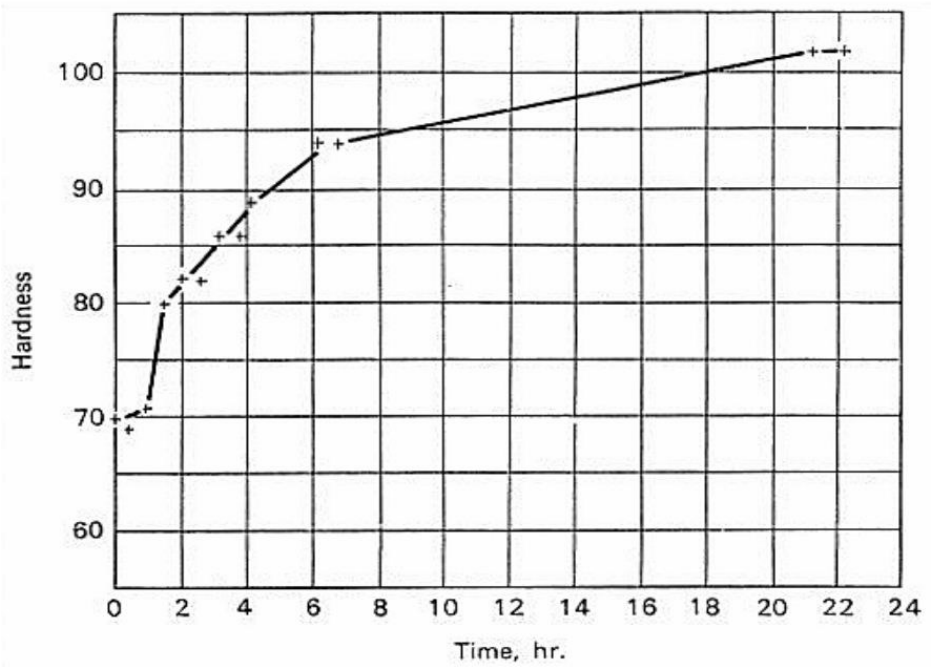

Fig. 1: The first age hardening curve of Duraluminum published by Alfed Wilms
[I. Polmear, Light Alloys - From Traditional Alloys to Nanocrystals, 4th ed. Oxford: Butterworth-Heinemann, 2006]

2.2 Solution heat treatment

However before natural aging occurs solution heat treatment needs to be applied.
Natural aging is achieved by the decomposition of a supersaturated solid solution (SSSS) through a variety of phase transformations and formation of fine precipitates.
During Solution heat treatment a materials is heated to a certain temperature T_a and after a holding time that depends on many parameters the material is quenched in water, oil, etc.
Through heating to T_a above the solvus and below eutectic temperature the solute atoms can form a homogeneous phase as illustrated.
During quenching the material is cooled to temperature T_b or T_c as in fig. 2.
After the heat treatment a supersaturated solid solution is present. Through approaching a lower Gibbs free energy this solution is decomposed after time by e.g. formation of precipitates that increase the strength.

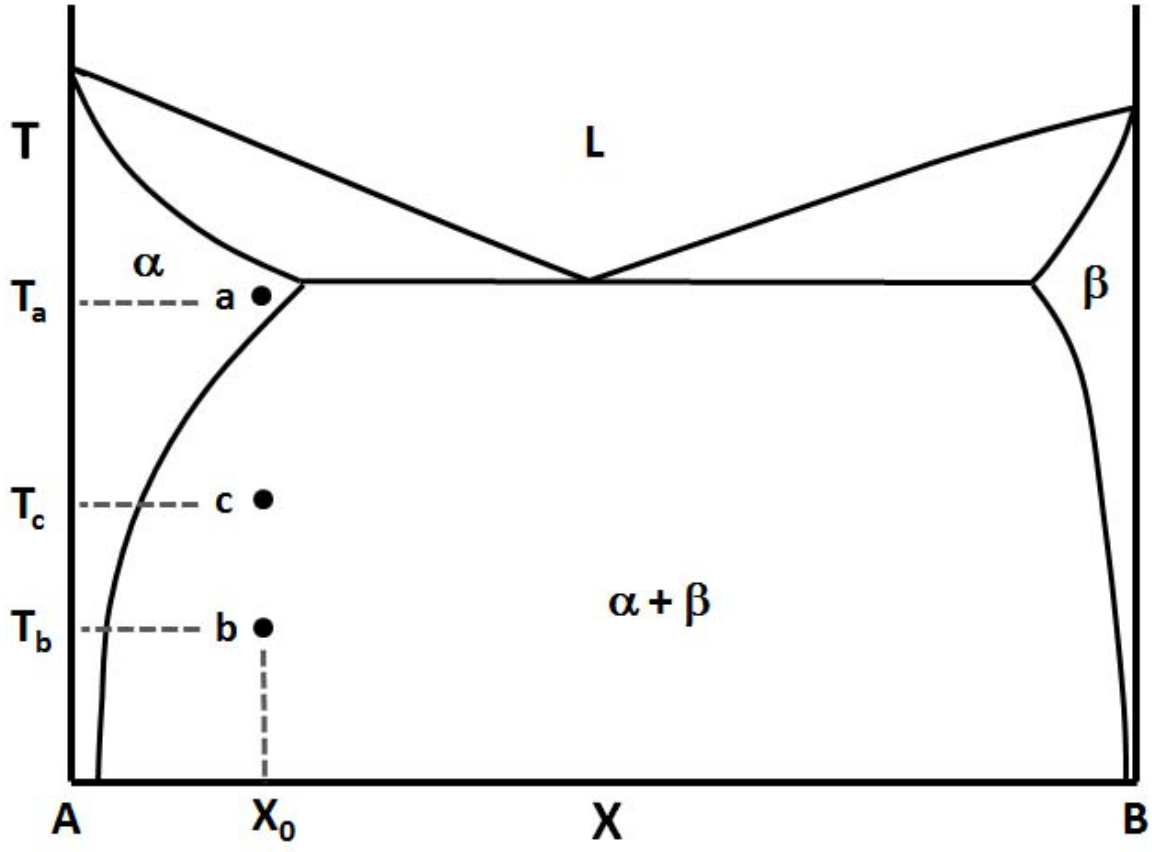

Fig. 2: Typical phase diagram for aluminum alloy heat treatment

2.3 Natural aging and artificial aging

After solution heat treatment and quenching either natural aging or artificial aging can be applied.
Natural aging is the aging at room temperature.
Artificial aging is done at elevated temperatures and most common for engineering aluminum alloys.

Important research has been done to suppress the effect of natural aging in order to improve mechanic properties.
One way is to add trace elements of Sn, In, Cd or Ag, etc.
For the alloy 6082 this is not a suitable technique because the content of Si and Mg is too high so that the trace elements cannot “block” the vacancies effectively.
Another way is pre-aging or interrupted quenching which is investigated in this thesis.
A possible thermal route was published by [Pogatscher et al., Influence of interrupted quenching on artificial aging of Al‑Mg‑Si alloys]

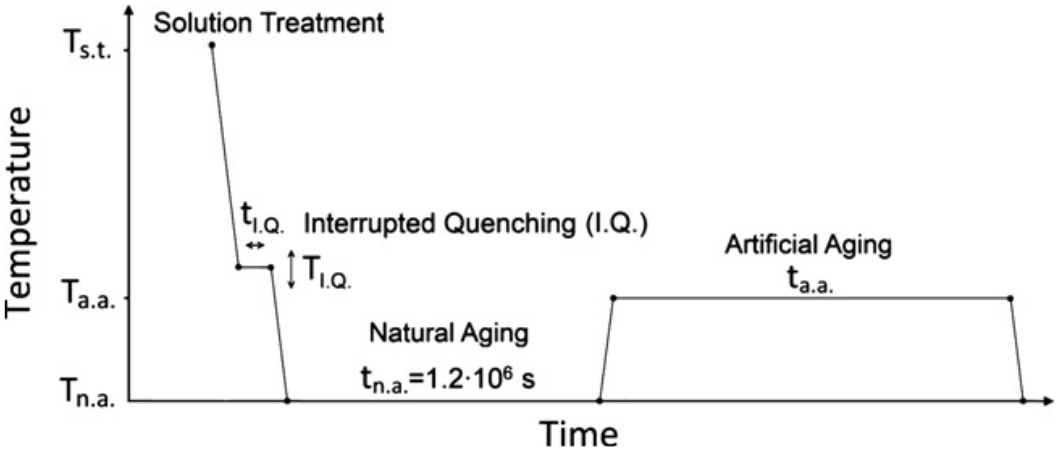

Fig.3: Heat treatment diagram with interrupted quenching

Interrupted quenching shown graphically in fig… was introduced as a new heat treatment strategy to study the effect of quenched-in vacancies on the nucleation of beta’’. IQ can form a dense distribution of beta’’ nuclei or reduce the remaining solute super-saturation. The effect of natural pre-aging on artificial aging is dependent on the quenched-in vacancies during nucleation.

Also a short term interruption of the quenching process can suppress natural aging.
Solute clustering during natural aging is also inhibited by IQ.
Due to the quenching procedure the vacancy concentration is reduced. Early stage of aging can be controlled by frozen-in vacancy concentration.
[Pogatscher et al., Process-controlled suppression of natural aging in an Al–Mg–Si alloy]
Beta’’ is the main hardening phase in AlMgSi alloys. When stored at room temperature atomic clusters are formed. GP-I zones are the first type of precipitates created in this alloy. When annealing temperature is higher than 125 °C beta’’ forms from pre-beta’’ precipitates. The atomic clusters that form during storage at RT inhibit the nucleation of pre-beta’’ precipitates.
[Marioara et al., The influence of temperature and storage time at RT on nucleation of the β’’ phase in a 6082 Al–Mg–Si alloy]

2.4 Precipitates and material

All the material used in this thesis came from the same extruded cups of 5 different aluminum alloys. The 6xxx alloy series is a wrought alloy and is heat-treatable. After the material has been homogenized at 535 °C which is a process meant to evenly distribute the alloying components the

material will be supersaturated with Mg and Si. Afterwards different natural aging and artificial aging conditions are applied.
The 6xxx aluminum alloys contains magnesium and silicon and get its strength from needle shaped precipitates formed during ageing. [Takeda M, Ohkubo F, Shirai T, Fukui K. Stability of metastable phases and microstructures in the ageing process of Al–Mg–Si ternary alloys [Journal Article]]
Manganese is also present to prevent recrystallization subsequent to solutionizing by pinning the grain boundaries, which is done by the manganese precipitates forming alpha dispersoids during homogenization.
To be able to get these precipitates, the material is first solutionized to bring silicon and magnesium into solid solution, that will later help form the wanted precipitates by becoming supersaturated when the material is quenched. Silicon has a lower solubility and goes out of the solid solution and forms the Si-clusters at quenched positions. The magnesium will then diffuse towards these clusters.
If the material is not quenched, but rather cooled down in room temperature, the desired precipitates will be lost as they diffuse into the equilibrium state called beta-particles, which has is a Mg_2Si structure. After quenching, the material is age hardened, which causes Guinier-Preston zones (GP-zones) to be formed before the beta" particles are formed. [Marioara CD, Andersen SJ, Jansen J, Zandbergen HW. Atomic model for GP-zones in a 6082 Al–Mg–Si system [Journal Article]. Acta Materialia]

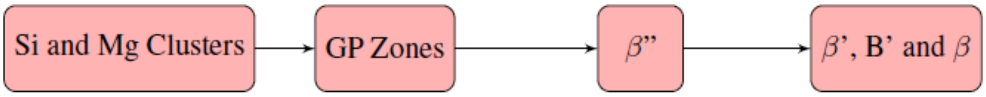

Fig. 4: Evolution of precipitate microstructure in 6xxx alloys

The beta"-particles are the wanted precipitates. Beta'' precipitates will grow in
<1 0 0> directions to block dislocations from the {1 1 1} slip plane. They are the ones that will give the highest hardness, and they occur at T6. Beta" are metastable particles approximately on the form Mg5Si6 and contains about 20% aluminum.
[Hasting HS, Frøseth AG, Andersen SJ, Vissers R, Walmsley JC, Marioara CD, et al. Composition of beta" precipitates in Al–Mg–Si alloys by atom probe tomography and first principles calculations [Journal Article]. Journal of Applied Physics. 2009;106(12):123527]
During over aging the beta" particles form other particles such as B', beta' and beta (equilibrium phase).
There are two popular theories about the formation of the over aged precipitates.
Site transformation theory assumes that particles keep transforming from beta'' to beta' and so forth.
Whereas another theory assumes that beta'' dissolves, nucleates and thus forms the over aged precipitates.
[Ryen Ø, Holmedal B, Marthinsen K, Furu T. Precipitation, strength and work hardening of age hardened aluminum alloys [Journal Article]. IOP Conference Series: Materials Science and Engineering. 2015;89(1):012013]

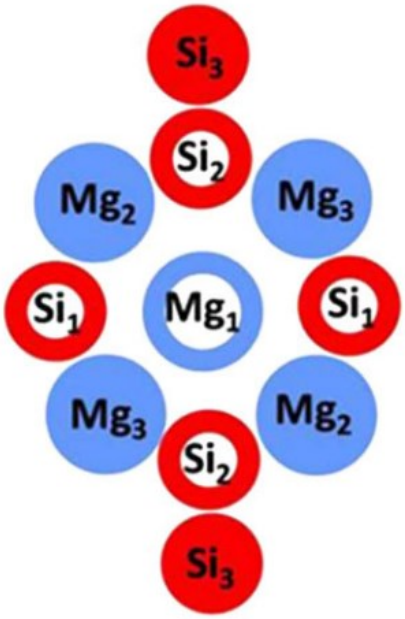

Fig. 5: Model of atomic positioning in a beta" particle with the formula Mg_5Si_6
[Ninive PH, Løvvik OM, Strandlie A. Density Functional Study of the beta" Phase in Al-Mg-Si Alloys [Journal Article]. Metallurgical and Materials Transactions]

3. Experimental procedures

3.1 TEM sample preparation

To prepare suitable TEM samples it is necessary to cut out small slices of the material with further grinding and polishing to a thickness of 0,1 mm.

In order to have a high probability to see grains in the <100> zone axis the transmission of electrons through the sample should be in extrusion direction. So half rings with a thickness of 2 mm were cut out of the sample cup.

Fig. 6: Sample cup with cut-out half rings

Fig. 7: Finished disk samples before electropolishing

These half rings (fig. 6) were ground and polished to a thickness of 0,3 mm. Then disks were punched out of the polished half ring segments.

The disks with a thickness of about 0,3 mm are polished to their final thickness of 0,1 mm and ready for electropolishing.

The electropolishing was done in a Struers Lectropol-5, using an A2 electrolyte (methanol and nitric acid) at a temperature of -25 °C.

3.2 Analysis of TEM images

All of the TEM research was done with a Jeol JEM 2100 - LaB6 microscope at NTNU Trondheim. From each condition about 5 images were recorded, also for each image an EELS (electron energy loss spectrum) was recorded to calculate the thickness at this position.

Measurement of precipitate length

For the measurement of the precipitate length the software ImageJ was used. After measuring all precipitate lengths it was possible to have a list with all lengths counted.

With the data from the analysis the average precipitate length and a distribution of lengths could be calculated.

Measurement of precipitate cross sections

Also the measurement of the precipitate cross sections was done with ImageJ. Here the area of the precipitates in zone axis is the measured value. The measured cross sections were used for statistics.

Measurement of sample thickness

For the calculation of the volume fraction it was necessary to know the thickness of the sample where the picture was taken. This was done by the analysis of the EELS spectrum.

$$d = \lambda \times \ln \frac{e_{tot}}{e_{0loss}}$$

λ is the mean free path, which is 126 nm for aluminum

e_{tot} is the total number of electrons transmitted through the sample

e_{0loss} is the number of electrons without energy loss

The analysis to count the sum of total and zero loss electrons is done by program DigitalMicrograph.

Correction of precipitate length

In order to have exact orientation in zone axis the sample holder in the TEM needs to be tilt. Therefore the measured precipitate length l_m needs to be corrected with this formula.

$$l = \frac{l_m}{1 - \frac{l_m}{t} \times \cos 45° \tan \theta}$$

l is the corrected precipitate length
l_m is the measured precipitate length
t is the sample thickness calculated with EELS
θ is the average tilt angle

$$\theta = \cos^{-1}(\theta_x \times \theta_y)$$

θ_x and θ_y are the TEM tilt angles in x and y direction

Calculation of precipitate density per volume

$$\rho = \frac{3 \times N}{A \times (t + l)}$$

ρ number density
N number of needles in [100] zone axis
t thickness
l corrected precipitate length

Calculation of volume fraction

$$VF = \rho \times CS \times l_m$$

ρ number density per volume
CS average cross section area
l_m average measured length

3.3 Tensile testing

In order to measure the tensile properties of the different states and alloys tensile specimen were worked out of the specimen cups with a CNC machine

Three samples per condition were extracted from each cup in order to have more confidence in the values measured. In total 64 conditions were tested. For the testing a Zwick/Roell Z010 tensile testing machine was used.

The values measured were tensile strength R_m, yield strength R_{p02}, elongation to fracture and uniform elongation.

Fig.8: Sample cups

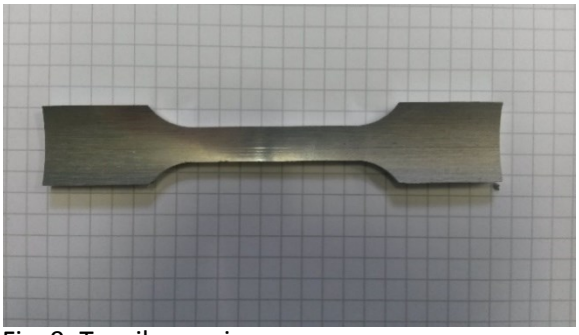

Fig. 9: Tensile specimen

Rolled specimen

In order to investigate the effect of predeformation by rolling samples were cut out of the cups and then rolled with a deformation range from 8 to 12 percent. One week of natural aging was applied after and before deformation followed by artificial aging.

Afterwards tensile specimen were produced by CNC machining to compare the mechanical properties of the rolled specimen.

3.4 Corrosion sample preparation and testing

Sample preparation

The sample cup is positioned in the band saw and the bottom is removed. The height of the bottom part is approximately 15 mm.
The part is 60 mm in diameter and needs to be cut in two halves for further sample preparation. The smaller half is then used for the corrosion testing.

Preparation of corrosion test

For the identification of the samples after the corrosion test it is necessary to engrave the number of each sample.
Before the corrosion test the cut cross section needs to be prepared with grinding paper P180.
Afterwards the samples are cleaned with acetone and ethanol.
The samples need to be weighed before and after the corrosion test to calculate the loss of mass.

Composition of corrosion test solution:
1000 ml H2O
20 g NaCl
100 ml conc. HCl (25 %)

Volume of the solution should be 8-10 ml per cm^2 of sample surface.

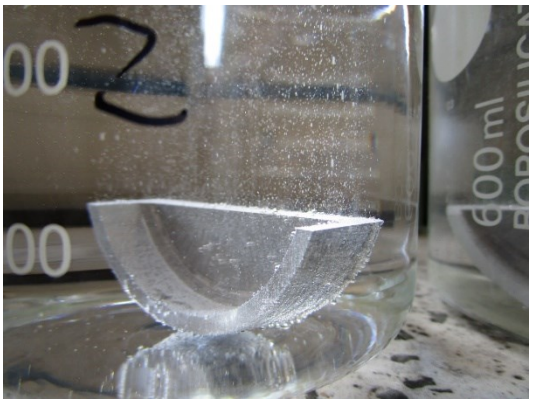

Fig. 10: Sample in corrosion solution

The radial part of the sample is positioned on the bottom as seen in fig. 10.

After 2 hours in the solution the samples are taken out and cleaned with water to inhibit further corrosion.
After the samples are dried, the mass is measured to calculate loss of mass.

Metallographic specimen

After the corrosion test a small slice of the sample is cut off to make a metallographic specimen.
The size of the part should be small to easily embed it in polymer mass.
The cut cross section should be on top of the finished specimen.
After embedding the specimen is ground (P320, P300, P1200) and polished with diamond suspension (9µm, 3µm, 1µm) to 1 µm.

Afterward the finished specimen is analyzed in the light microscope at three positions with magnification 20x.

T3 is the position with 3 mm in thickness
TR is the position with curvature
T5 is the position with 5 mm in thickness

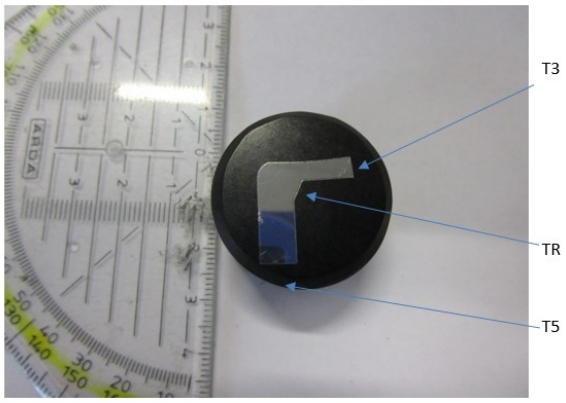

Fig. 11: Areas of interest

4. Results & Discussion

4.1 Results of tensile testing

When comparing 10 minutes and 1 week of natural aging, the 1 week of natural aging is improving ductility in all alloys, with the exception of 6066, where only the strength increases. For 6261 both ductility and strength are improved. The 6082low experiences a decrease in strength in the 1 week condition.

In general, the 10 minutes of natural aging and the PA_B conditions produce the worst ductility. These conditions have similar respective strength.

The best ductility is given by the PA_C conditions, but the strength is lowest. In this case alloys 6261 and 6066 produce the best combination of strength and ductility.

Conditions PA_D are best when strength and ductility are considered, for most of the alloys. The second best conditions are the 1 week of natural aging.

Condition PA_A has similar, or slightly better ductility than the 10 minutes of natural aging and PA_B, and similar strengths, except alloy 6261, where the strength increase is highest.

As a general remark, any pre-aging treatment (except PA_B) seems to improve ductility, but the best results are obtained when a 1 week of natural aging is included (meaning the conditions 1week NA, PA_C and PA_D).

The rolled specimen showed a much lower elongation than the non-deformed ones due to the predeformation.

For the conditions with one week of natural aging + deformation the highest values for yield stress were observed.
For the samples that were deformed right after solution heat treatment and quenching both ductility and yield stress were the lowest for all conditions.

The analysis of the hardening coefficient n showed significant difference between 9 and 14 hours of artificial aging. The conditions with 9 hours of artificial aging have a higher UTS/YS ratio, resulting in a higher value for n.

The mechanical properties are compared to TEM parameters later on.

Tab. 1: Abbreviations for pre aging treatments

Pre aging	Condition
PA_A	10 minutes + 3 hours at 140°C + 10 minutes
PA_B	10 minutes + 30 minutes at 100°C + 10 minutes
PA_C	10 minutes + 3 hours at 140°C+ 1 week
PA_D	10 minutes + 30 minutes at 100°C + 1 week

4.2 TEM results

4.2.1 TEM analysis of alloy 6082high

Alltogether 8 different conditions of this alloy were investigated in TEM:

- 10M-9h
- 10M-14h
- 1W-9h
- 1W-14h
- PA_A -9h
- PA_A -14h
- PA_D -9h
- PA_D -14h

The aim was to analyse the precipitate statistics (length and cross section) and therefore evaluate its correlation with the mechanic properties.

Microstructure

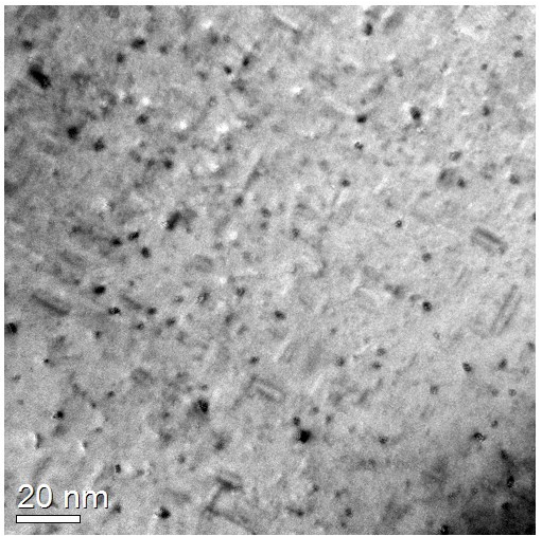

Fig. 12: TEM image 6082↑- PA_A-9h

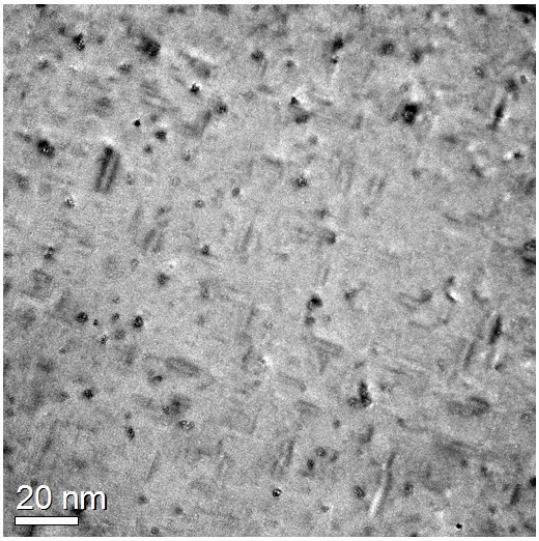

Fig. 13: TEM image 6082↑- PA_A-14h

The microstructure consists of many small needle shaped precipitates. Many of them are similar to beta'' but only a fraction are real beta'' precipitates as can be seen in fig. 12 and 13.

The condition with 140°C of pre-aging (PA_A) showed a small precipitate length and cross section. The pre-aging at 140°C seems to create many precipitates with small lengths and cross sections.

TEM values and mechanical properties

By comparing artificial aging time it can be concluded that particle length and cross section increase with aging time due to particle coarsening. The highest needle length and also cross section area was ovserved for the conditions with 10 minutes of natural aging.

The condition with pre aging of 3 hours at 140 °C (PA_A) show the smallest needle lengths and cross sections with a fairly high number density. For the calculation of the volume fraction many parameters influence the result so the error is quite high.

The PFZ width for all conditions was between 58 and 109 nm. Condition PA_D-14 showed the highest PFZ width of all conditions. When comparing PFZ width to mechanical properties the correlation was small. In the table 2 we can see that yield strength decreases with increasing average PFZ width. The conditions with pre aging showed a slightly larger PFZ width for 14 hours artificial aging.

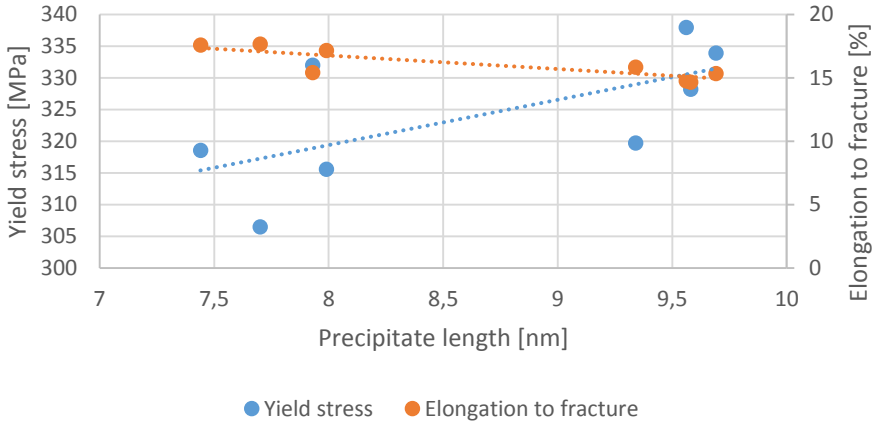

Fig. 14: Precipitate length compared to yield stress and elongation to fracture

Generally it can be seen that with longer needles the yield strength increases. Still there is not a clear trend for the first cluster between 7 and 8 nm needle length as seen in fig. 14.

This analysis clearly shows that ductility is slightly higher with smaller needles. Thus longer precipitates reduce elongation to fracture.

The cross section area of the needles correlates to yield strength similarly as the needle length. A larger cross section can block more dislocations and therefore raise yield strength.

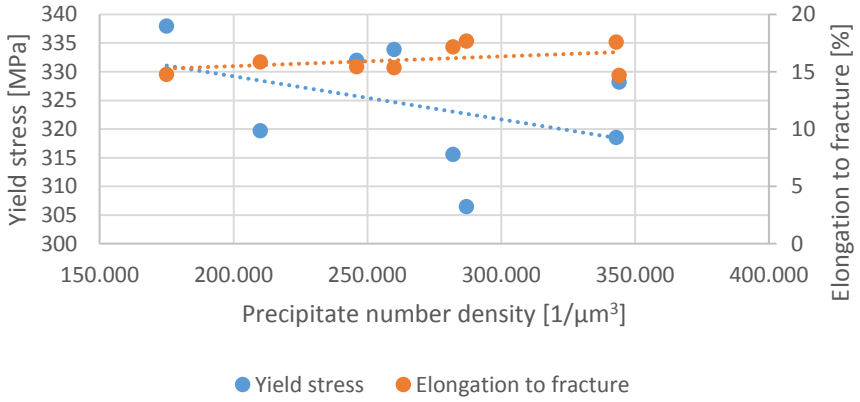

Fig. 15: Number density compared to yield strength and elongation to fracture

It can be observed that yield stress slightly decreases with increasing number density. This might indicate that the number of precipitates has a strong influence on mechanical properties. The highest yield stress in fig. 15 is reached with the lowest number density.

It can be observed that ductility is slightly increasing with a higher number density. However the correlation is not as high because some values are far out of the trend.

4.2.2 TEM analysis of alloy 6060

For this alloy the condition 6060-10M-14 was analysed in the TEM. This alloy has a low level of alloying elements such as copper, manganese, etc.

Therefore we expect a low density of precipitates. For this alloy only one condition was analyzed in the TEM.

Microstructure

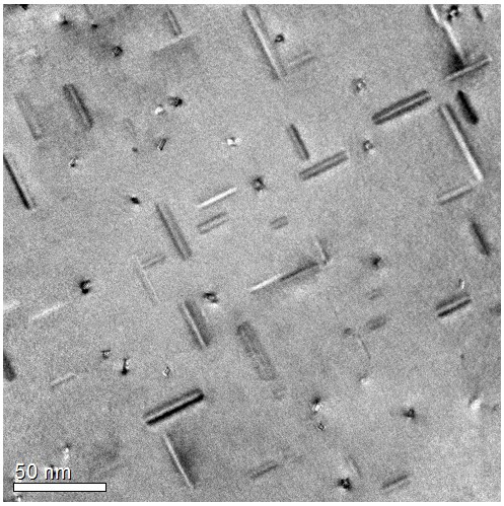

Fig. 16: TEM image of condition 6060-10M-14

It can be seen that there are fewer precipitates which have a larger cross section and length compared to the other alloys 6082 and 6066. The analysis confirms that the measured length and cross sections are larger. Also the number density is about a tenth compared to other alloys. The PFZ width is the highest measured for all alloys investigated.

4.2.3 TEM analysis of alloy 6066

In total two conditions (10 minutes natural aging) of this alloy were investigated in TEM:

- 6066-10M-9
- 6066-10M-14

This alloy has a high level of alloying elements, especially a high copper content.

Microstructure

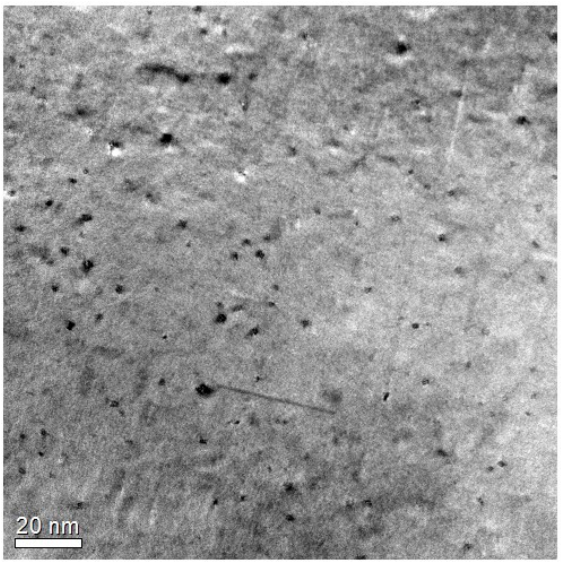

Fig. 17: TEM image 6066-10M-9

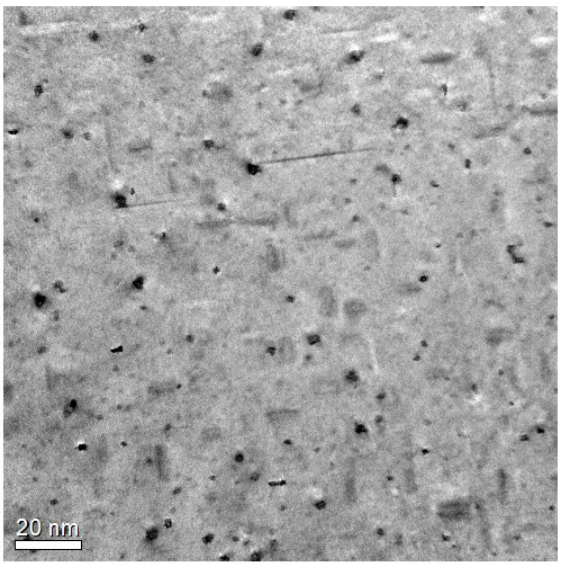

Fig. 18: TEM image 6066-10M-14

In comparison to the other alloys here additionally L’ precipitates can be observed. These precipitates have a small cross section and are relatively long compared to the other ones.

Also the precipitates in this alloy are quite small and the number density is high.

It can be ovserved that both needle lengths and cross sections grow with additional artificial aging time as expected. The condition with 9 h AA shows many very small precipitates. With longer artificial aging time particle coarsening is oberserved.

It can be ovserved that both needle lengths and cross sections grow with additional artificial aging time as expected. The condition with 9 h AA shows many very small precipitates. With longer artificial aging time particle coarsening is oberserved.

4.2.4 TEM results comparison of alloys 6082high, 6060 and 6066

Alltogther 11 conditions were analysed in the TEM. The alloy 6082high had the highest priority. Also alloys 6060 and 6066 were analysed in the TEM.

Table.2:.TEM properties and mechanical properties

Condition	<L> [nm]	<CS> [nm^2]	VF [%]	ρ [1.000/µm^3]	PFZ width [nm]	R_m [MPa]	$R_{p0.2}$ [MPa]	A_{40mm} [%]	A_g [%]
6082↑-10M-9	9 ± 2	6 ± 4	1,2 ± 0,1	210 ± 10	71 ± 12	379 ± 1	320 ± 1	15,8 ± 0,6	11,0 ± 0,2
6082↑- PA_A-9	7 ± 3	4 ± 2	1,1 ± 0,1	343 ± 17	71 ± 12	387 ± 1	319 ± 1	17,6 ± 0,5	11,9 ± 0,1
6082↑-1W-9	8 ± 2	3 ± 2	0,8 ± 0,2	287 ± 61	77 ± 5	381 ± 1	307 ± 1	17,7 ± 0,2	12,5 ± 0,3
6082↑- PA_D-9	8 ± 3	5 ± 2	1,3 ± 0,1	282 ± 5	80 ± 3	385 ± 1	316 ± 1	17,2 ± 0,5	12,3 ± 0,1
6082↑-10M-14	10 ± 3	7 ± 4	1,0 ± 0,1	175 ± 14	62 ± 4	387 ± 1	338 ± 3	14,8 ± 0,3	9,8 ± 0,1
6082↑- PA_A-14	8 ± 3	5 ± 2	1,2 ± 0,1	246 ± 18	75 ± 10	393 ± 1	332 ± 1	15,4 ± 0,1	10,8 ± 0,1
6082↑-1W-14	10 ± 3	5 ± 3	1,0 ± 0,1	344 ± 25	68 ± 5	391 ± 1	328 ± 1	14,7 ± 0,3	11,1 ± 0,2
6082↑-PA_D-14	10 ± 3	6 ± 3	0,9 ± 0,1	260 ± 8	91 ± 10	391 ± 1	334 ± 1	15,4 ± 0,6	10,7 ± 0,3
6060-10M-14	21 ± 8	11 ± 4	0,6 ± 0,1	24 ± 1	155 ± 6	211 ± 2	184 ± 1	11,6 ± 0,1	6,2 ± 0,1
6066-10M-9	8 ± 6	3 ± 2	0,9 ± 0,1	337 ± 5	72 ± 2	413 ± 3	320 ± 4	17,9 ± 0,6	13,5 ± 0,2
6066-10M-14	10 ± 4	4 ± 2	1,1 ± 0,1	313 ± 13	85 ± 11	421 ± 1	335 ± 1	17,4 ± 0,7	12,7 ± 0,3

In order to relate mechanical properties to TEM properties certain parameters were compared in diagrams.

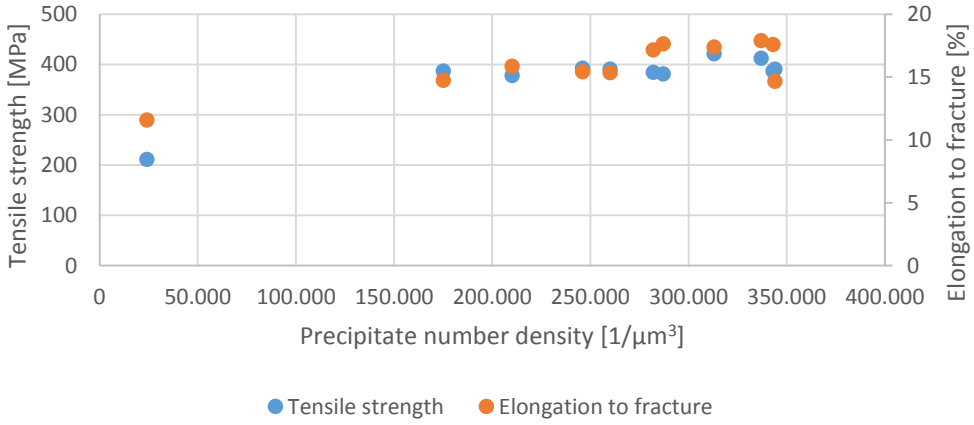

Fig. 19: Precipititate number density compared to tensile strength and elongation to fracture

There is only a slight correlation between tensile stress and number density of precipitates. But with a higher number density tensile stress tends to rise. It seems that tensile strength reaches a plateau as seen in fig. 19.

The relationship is similar to tensile stress, the difference between the stess values is even smaller for number densities between 150.000 and 350.000 1/µm^3.

There is a slight correlation between number density and elongation to fracture. It seems that with an increasing number of precipitates, elongation to fracture increases. Just one value is not in the trend as can be seen in fig. 19.

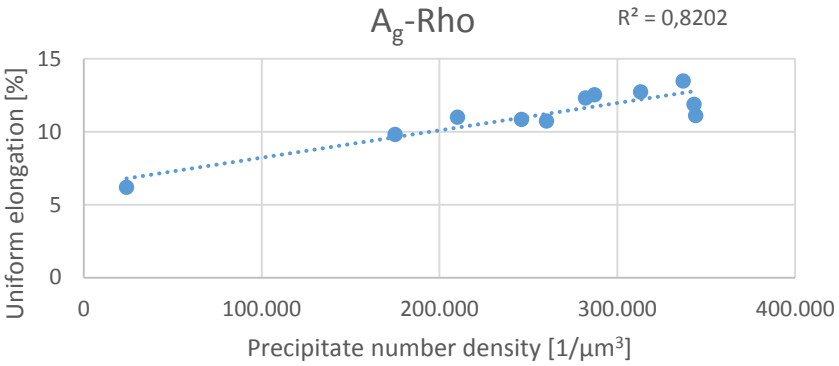

Fig. 20: Precipitate number density – uniform elongation

There is even a slightly higher correlation between number density and uniform elongation, just 2 data points are far out of the trend. The correlation with yield strength was lower.

Here it seems again that many precipitates increase the ductility. For example the alloy 6060 has a low number density and the smallest ductility of all alloys.

Comparison to other TEM parameters

When comparing properties such as volume fraction, precipitate length and cross section the correlation was poor.

We would expect a higher correlation with the volume fraction but this was not apparent as seen in fig. 21. The volume fraction takes into account number density, thickness, precipitate length and cross section. Thus a high error is possible.

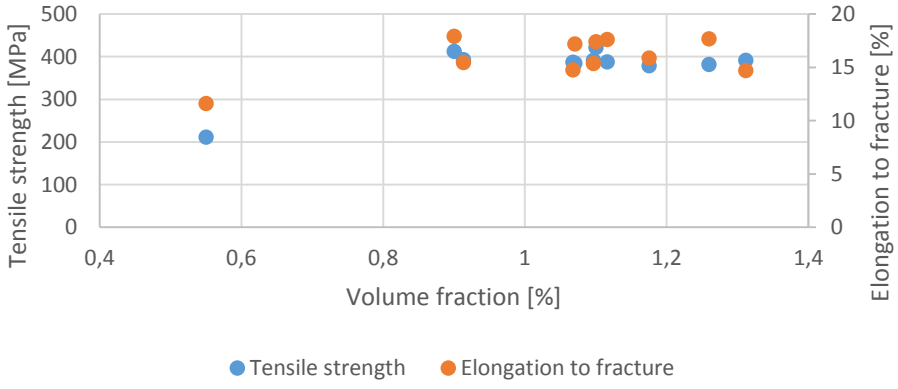

Fig. 21: Volume fraction compared to tensile strength and elongation to fracture

Therefore there is no clear trend for the relationship between volume fraction and mechanical properties.

Also when different alloys are compared the number density for the low alloyed is a much lower, so it makes no sense to compare precipitate length and cross section for different alloys.

4.3 Analysis of corrosion

The corrosion tests resulted in following values:

- mass loss for each condition
- penetration depth for each condition
- images in light microscope of each condition

Tab. 3: Average mass loss of alloys during corrosion test

Alloy	Avg. mass loss	Range
6261	1,27	1,02-1,56
6082 low	0,86	0,68-1,08
6082 high	0,60	0,51-0,77
6060	0,54	0,43-0,83
6066	1,16	0,95-1,35

In general the corrosion beahaviour depends on alloying elements and heat treatment. High alloyed aluminum is expected to show more corrosion than low alloyed.

The investigated allos show corrosion as expected with the exception that the high alloyed 6082 shows actually less corrosion than the low alloyed 6082 as seen in table 3.

In order to explain this exactly very detailed analysis would be needed. But according to Prof Erbe of NTNU the higher silicon content of the 6082 high might be the explanation for less corrosion. The Silicon might passivate the cathode when it forms grain boundary precipitates and thus inhibit intergranular corrosion.

The most important parameter is the copper content of the alloys. The most copper-rich alloys 6261 and 6066 show the hightest corrosion followed by 6082.

Mass loss / penetration depth

Following diagrams relate the mass loss to penetration depth. It can be seen that the alloys show different trends such as proportional dependence or clusters.

For the high alloyed 6082 the correlation between mass loss and penetration depth is less present than in the other alloys. It shows clustering in a certain area (fig. 24).

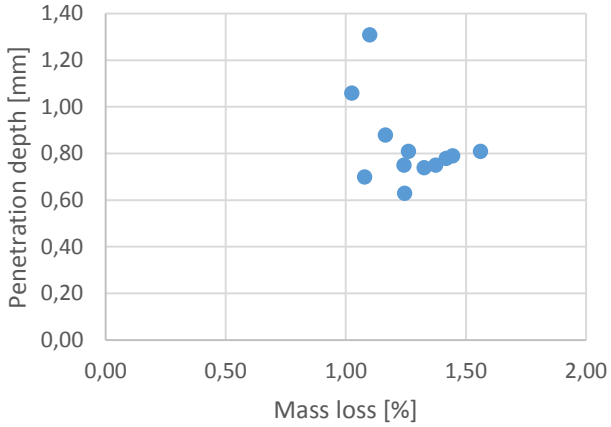

Fig. 22: 6261 Mass loss- penetration depth

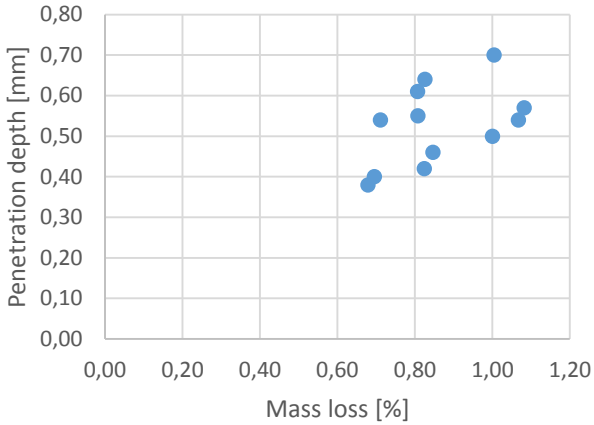

Fig. 23: 6082↓ Mass loss- penetration depth

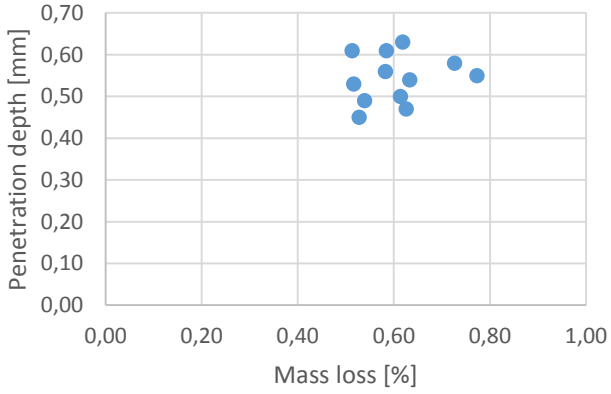

Fig. 24: 6082↑ Mass loss- penetration depth

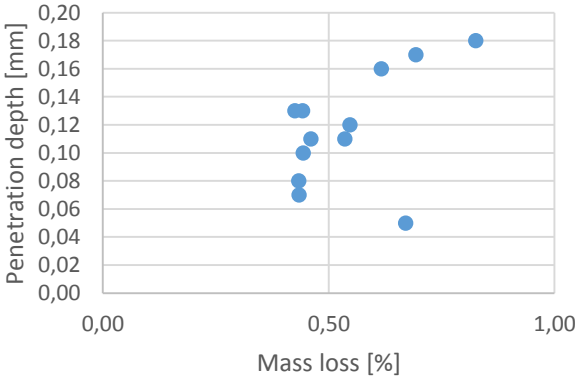

Fig. 25: 6060 Mass loss- penetration depth

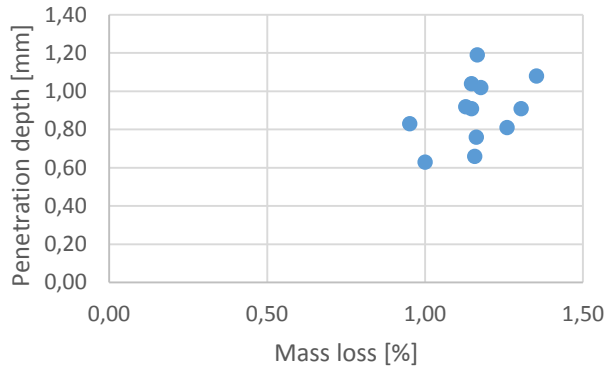

Fig. 26: 6066 Mass loss- penetration depth

Influence of artificial aging on corrosion

For this analysis the average mass loss for each alloy with 9 and 14 hours of artificial aging was calculated. It can be seen that mass loss slightly increases with longer artificial aging. This is caused by a change in size and composition of grain boundary precipitates.

The biggest increase in mass loss from 9 to 14 hours AA can be observed for alloy 6060 which has a low content of alloying elements.

Tab. 4: Comparison of average mass loss for 9 and 14 h AA

Alloy-AA	Average mass loss [%]	**Increase [%]**
1-9h	1,21	**8,3**
1-14h	1,32	
3-9h	0,84	**4,5**
3-14h	0,88	
4-9h	0,58	**6,5**
4-14h	0,62	
15-9h	0,47	**24,2**
15-14h	0,62	
17-9h	1,15	**2,5**
17-14h	1,18	

5. Summary of results

With increasing natural aging time ductility improved for most conditions (except alloy 6066), however tensile and yield strength slightly decreased.

The pre aging with 30 minutes at 100°C showed no improvement for mechanical properties.

Conditions with 3 hours at 140°C show high strength combined with an elevated ductility and might be of further interest.

The samples with one week of natural aging during solution heat treatment with quenching and predeformation showed the hightest yield strength but also the lowest ductility.

The most important parameters of the TEM investigations were precipitate length, cross section and number density. Alltogether 8 conditions of alloy 6082high, two conditions of alloy 6066 and one condition of 6060 were analysed.

All conditions of alloy 6082high showed similar values. The condition with pre aging at 140°C and 9 hours of artificial aging showed a relatively high number density combined with small precipitates (similar to beta'').

The lean alloy 6060 showed a low number density with longer and wider precipitates (beta'').

The copper-rich alloy 6066 showed the highest precipitate number density. The precipitate types in this alloy were beta'' and also L' due to the high copper content.

In order to check correlation between mechanical and TEM properties, different values were compared in diagrams.

The precipitate number density (TEM) showed a slight correlation with mechanical properties. The highest correlation was observed between uniform elongation and precipitate number density.

Concerning corrosion properties the most important parameter was the copper content of the alloys. Corrosion strongly depends on the composition of the grain boundary precipitates, which is influenced by many factors such as heat treatments and solute content. Also with longer artificial aging time the mass loss increases.

6. Appendix

TEM images

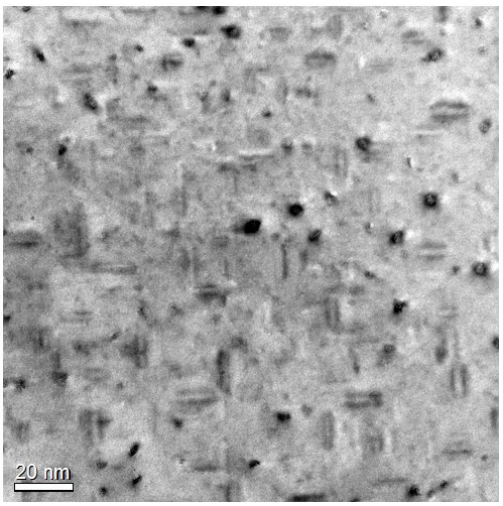

Fig. 27: TEM image 6082↑-10M-9

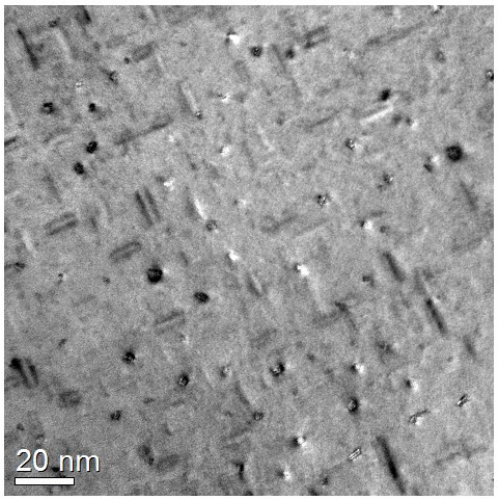

Fig. 28: TEM image 6082↑-10M-14

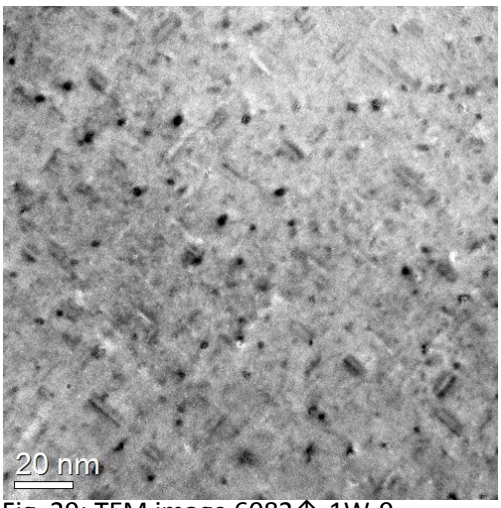

Fig. 29: TEM image 6082↑-1W-9

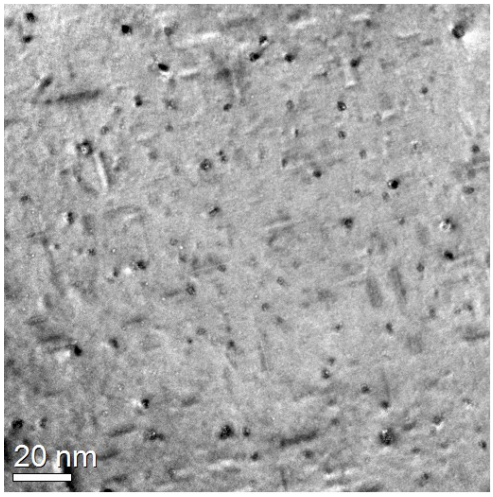

Fig. 30: TEM image 6082↑-1W-14

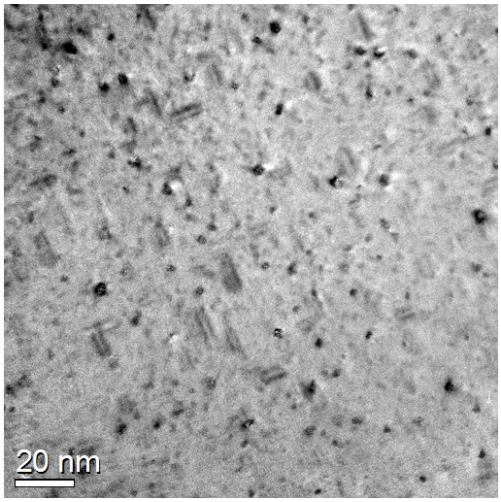

Fig. 31: TEM image 6082↑-PA_D-9

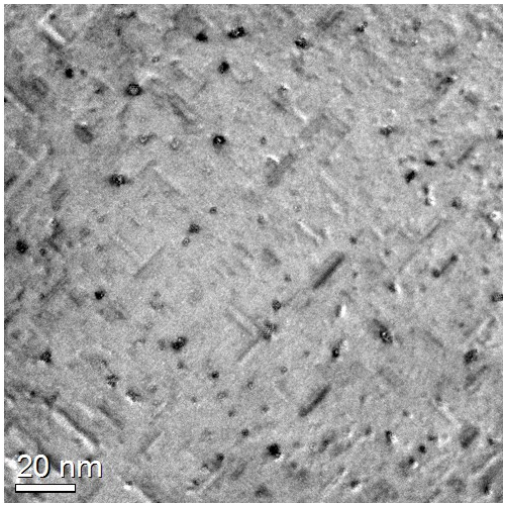

Fig. 32: TEM image 6082↑- PA_D-14

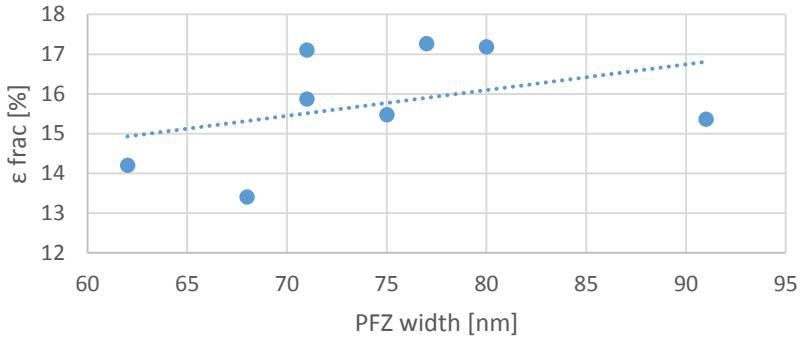

Fig. 33: PFZ width – Elongation to fracture 6082↑

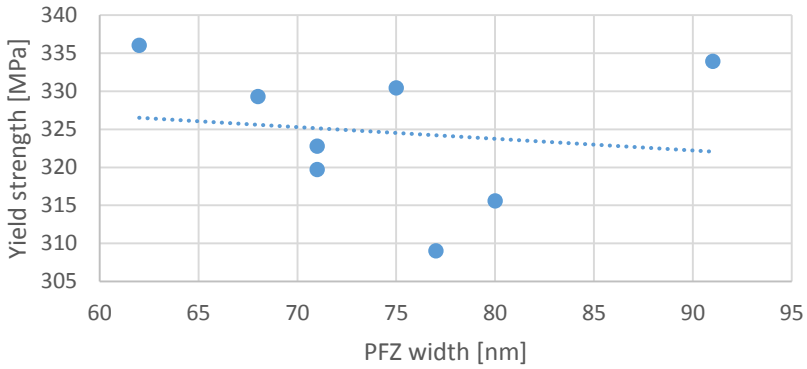

Fig. 34: PFZ width – Yield strength alloy 6082↑

Corrosion light microscope pictures of all conditions

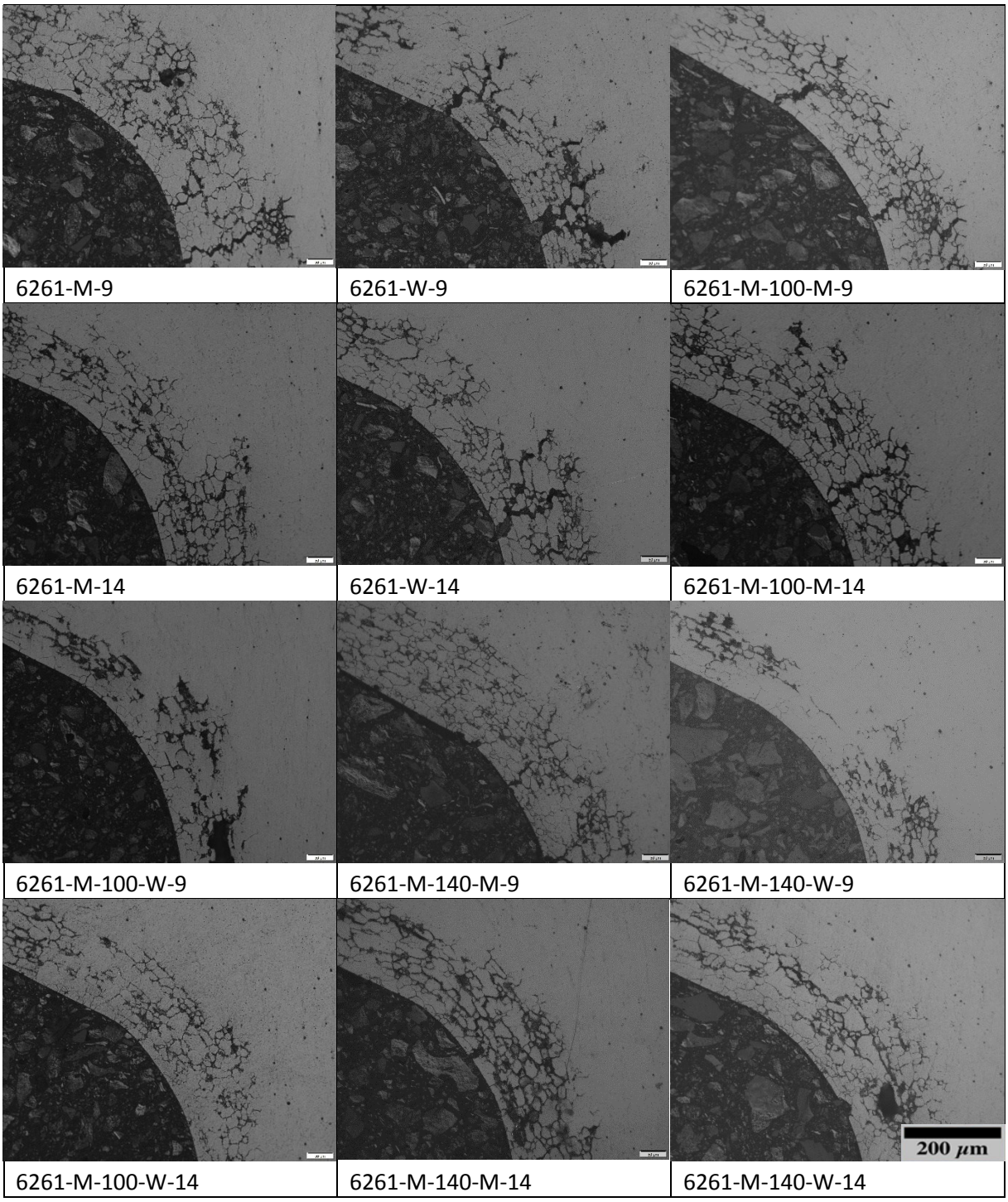

6261-M-9	6261-W-9	6261-M-100-M-9
6261-M-14	6261-W-14	6261-M-100-M-14
6261-M-100-W-9	6261-M-140-M-9	6261-M-140-W-9
6261-M-100-W-14	6261-M-140-M-14	6261-M-140-W-14

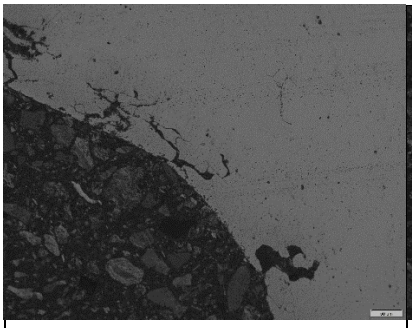	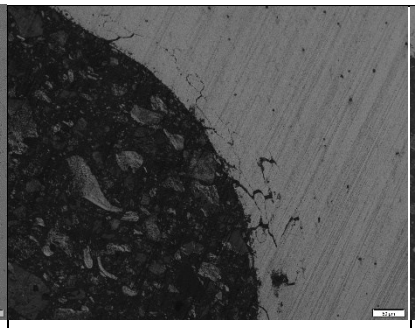	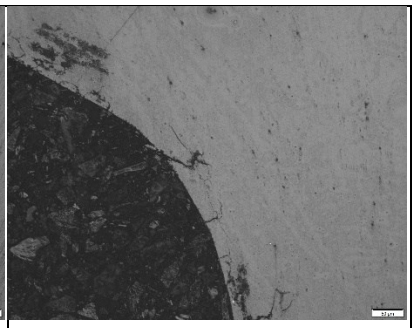
6082↓-M-9	6082↓-W-9	6082↓-M-100-M-9
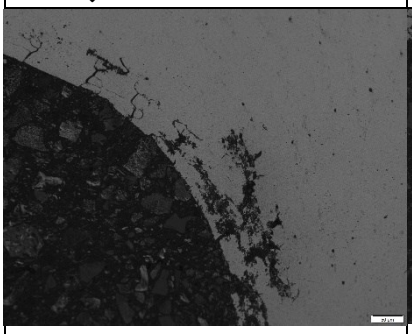	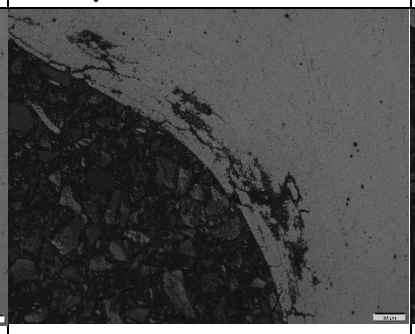	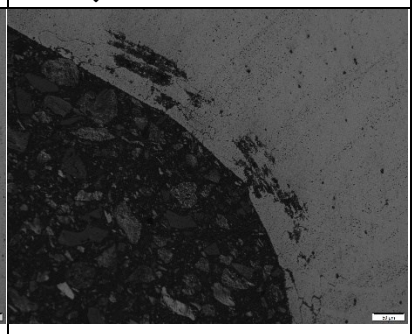
6082↓-M-14	6082↓-W-14	6082↓-M-100-M-14
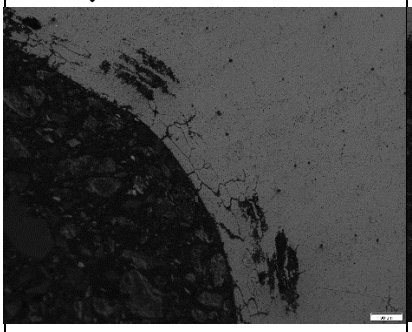	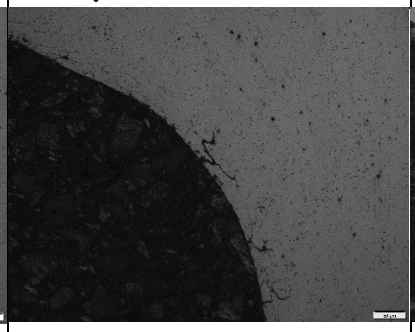	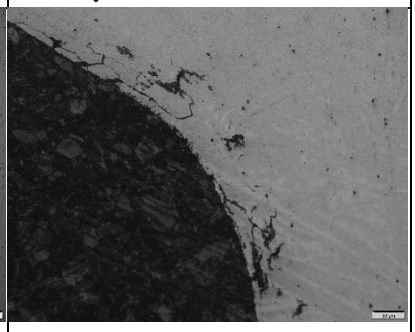
6082↓-M-100-W-9	6082↓-M-140-M-9	6082↓-M-140-W-9
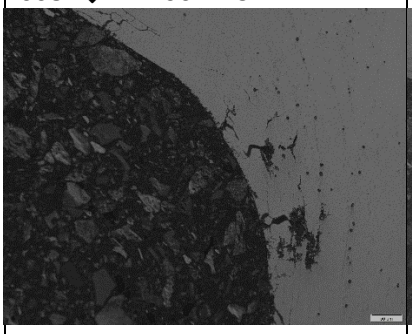	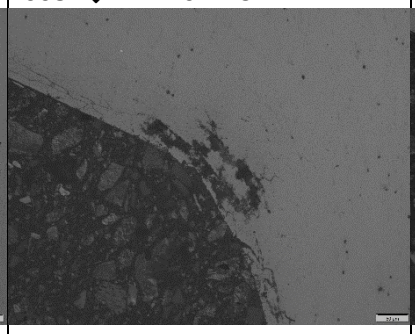	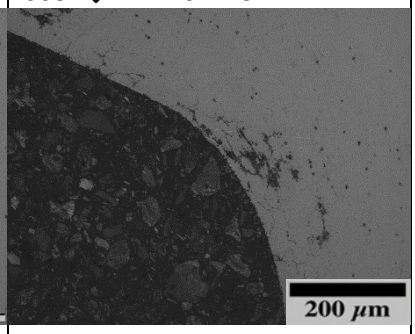
6082↓-M-100-W-14	6082↓-M-140-M-14	6082↓-M-140-W-14

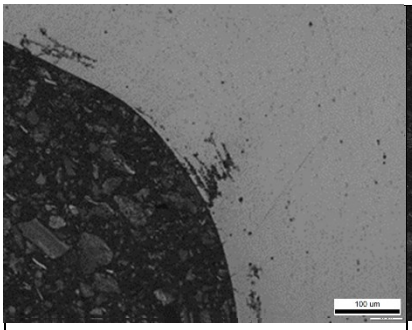	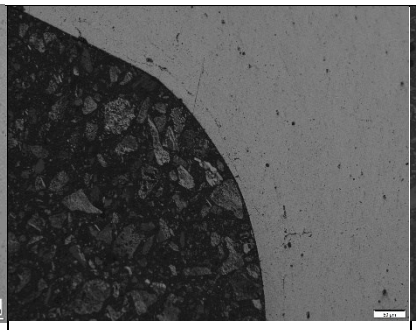	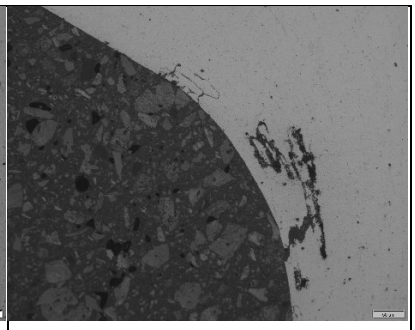
6082个-M-9	6082个-W-9	6082个-M-100-M-9
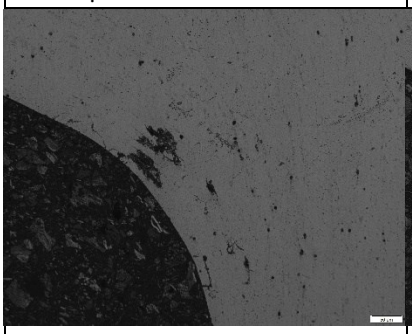	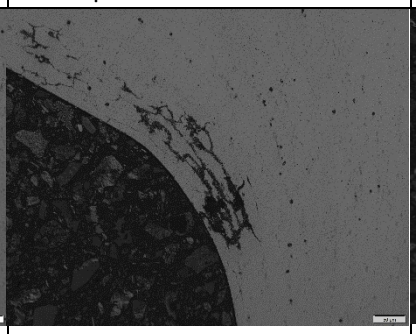	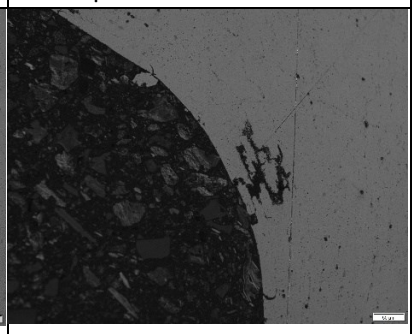
6082个-M-14	6082个-W-14	6082个-M-100-M-14
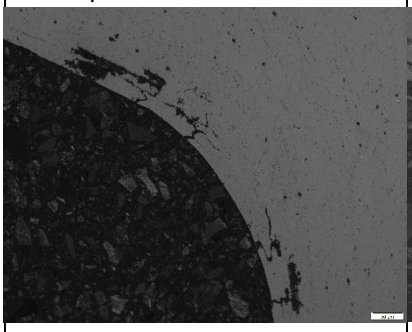	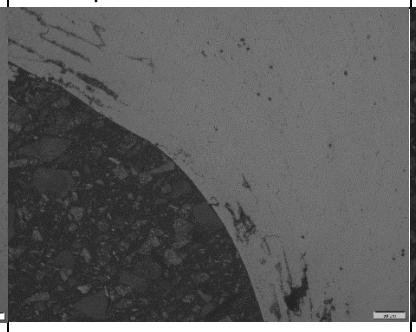	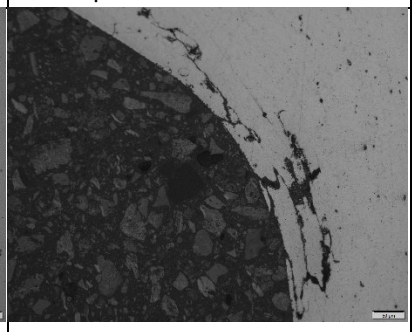
6082个-M-100-W-9	6082个-M-140-M-9	6082个-M-140-W-9
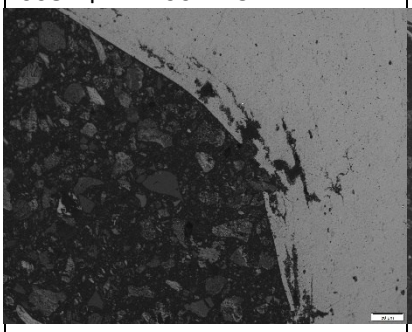	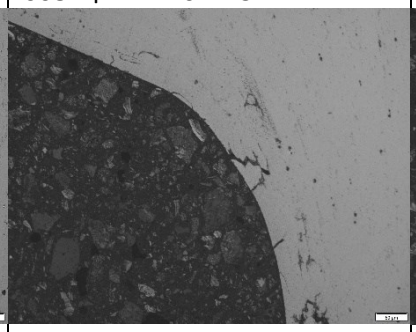	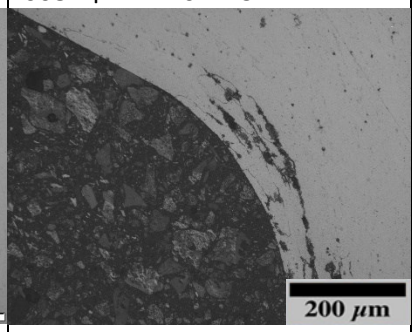
6082个-M-100-W-14	6082个-M-140-M-14	6082个-M-140-W-14

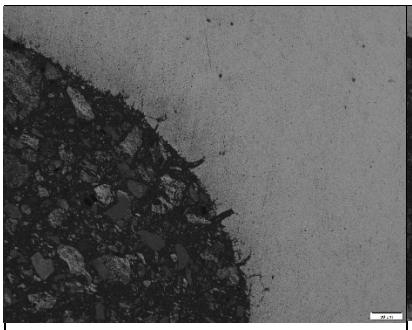	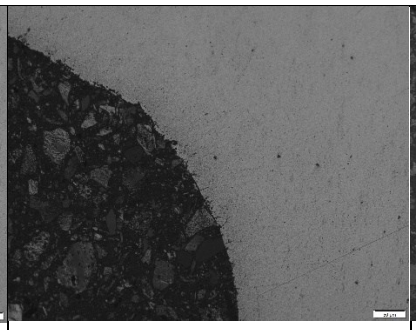	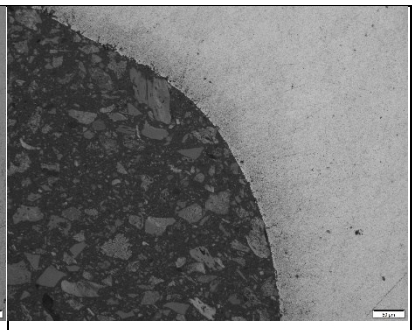
6060-M-9	6060-W-9	6060-M-100-M-9
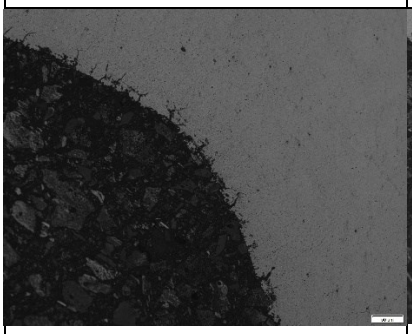	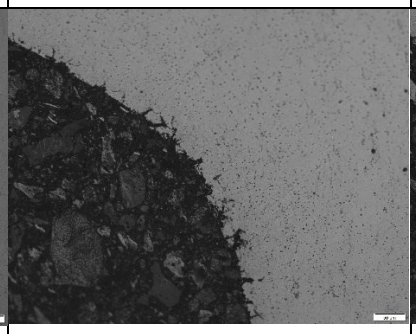	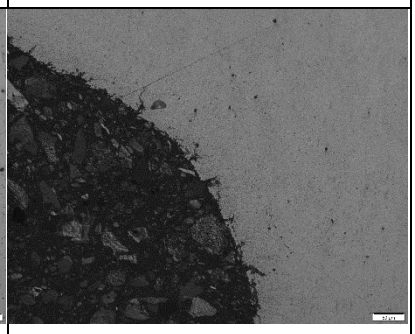
6060-M-14	6060-W-14	6060-M-100-M-14
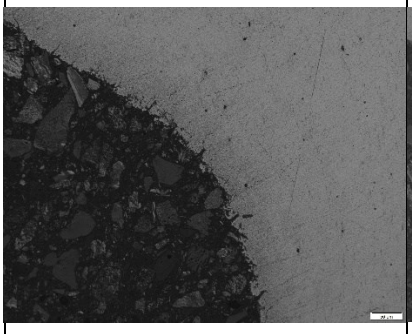	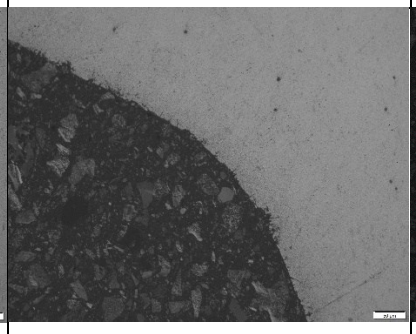	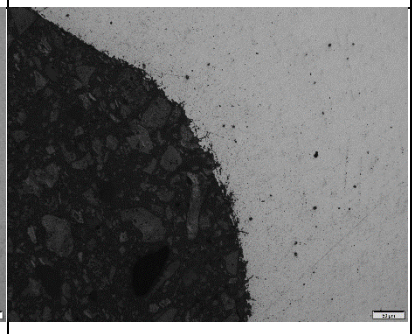
6060-M-100-W-9	6060-M-140-M-9	6060-M-140-W-9
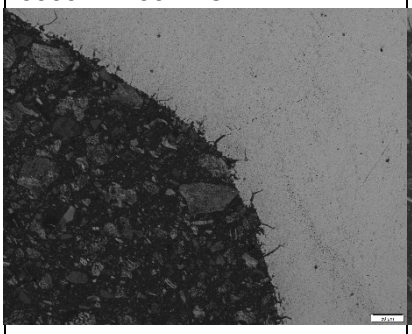	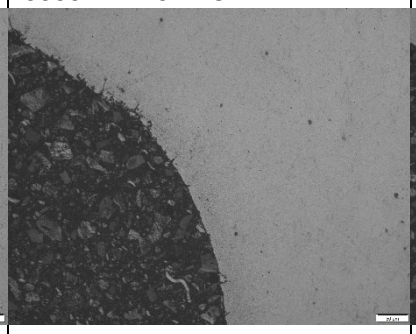	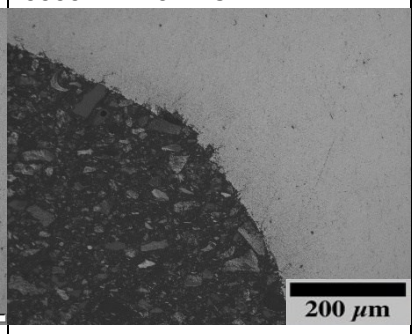
6060-M-100-W-14	6060-M-140-M-14	6060-M-140-W-14

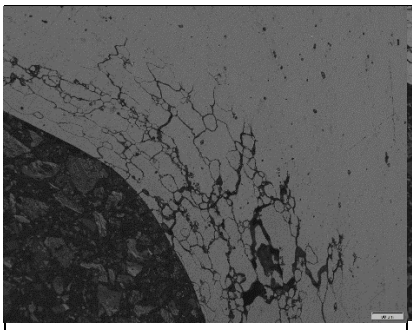	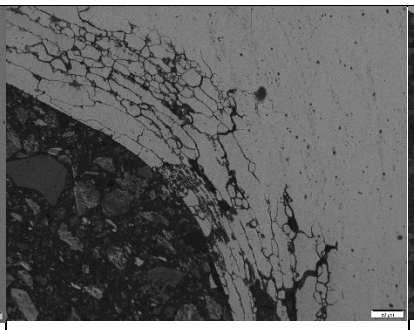	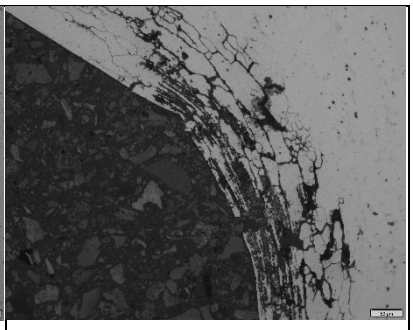
6066-M-9	6066-W-9	6066-M-100-M-9
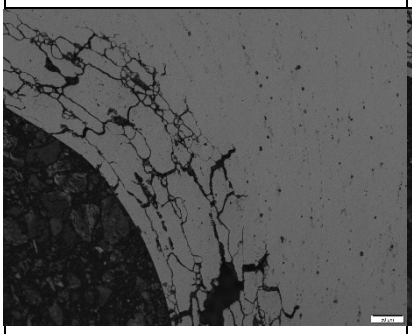	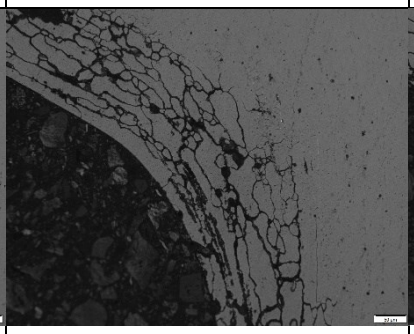	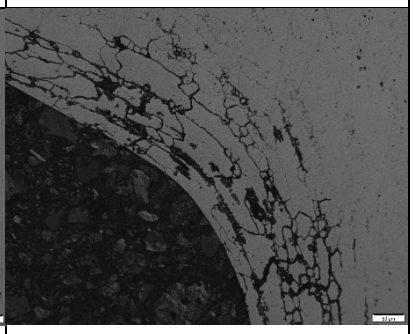
6066-M-14	6066-W-14	6066-M-100-M-14
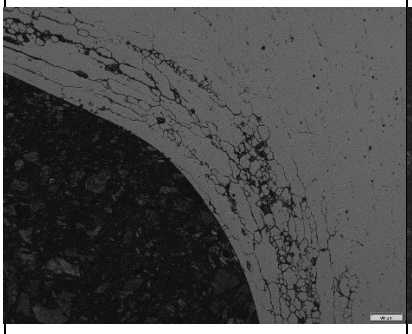	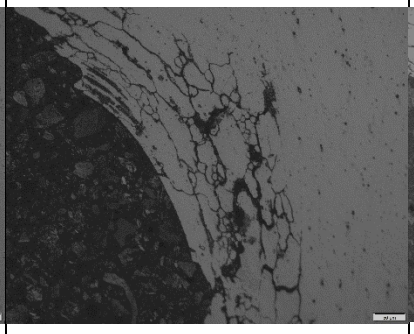	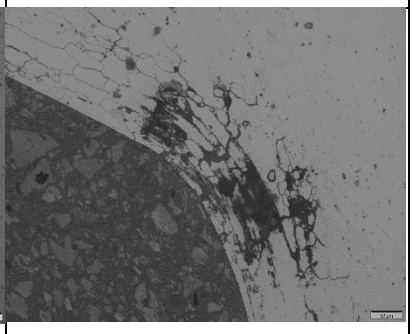
6066-M-100-W-9	6066-M-140-M-9	6066-M-140-W-9
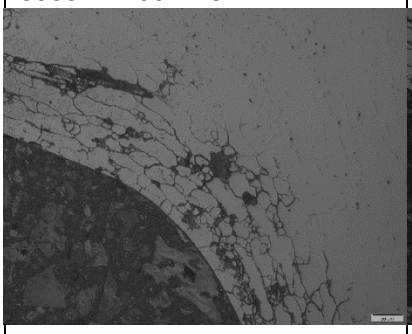	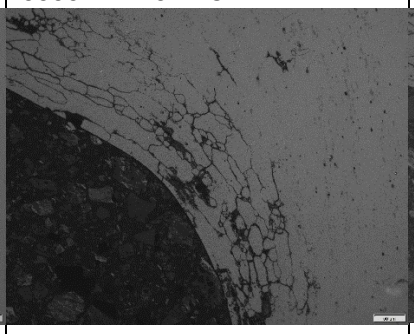	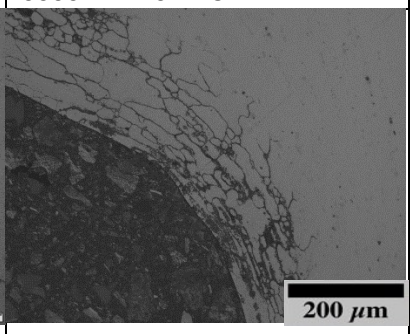
6066-M-100-W-14	6066-M-140-M-14	6066-M-140-W-14